



HAL
open science

Screening and polaronic effects induced by a metallic gate and a surrounding oxide on donor and acceptor impurities in silicon nanowires

Mamadou Diarra, Christophe Delerue, Yann-Michel Niquet, Guy Allan

► **To cite this version:**

Mamadou Diarra, Christophe Delerue, Yann-Michel Niquet, Guy Allan. Screening and polaronic effects induced by a metallic gate and a surrounding oxide on donor and acceptor impurities in silicon nanowires. *Journal of Applied Physics*, 2008, 103, pp.073703-1-5. 10.1063/1.2901182 . hal-00357380

HAL Id: hal-00357380

<https://hal.science/hal-00357380>

Submitted on 10 Feb 2022

HAL is a multi-disciplinary open access archive for the deposit and dissemination of scientific research documents, whether they are published or not. The documents may come from teaching and research institutions in France or abroad, or from public or private research centers.

L'archive ouverte pluridisciplinaire **HAL**, est destinée au dépôt et à la diffusion de documents scientifiques de niveau recherche, publiés ou non, émanant des établissements d'enseignement et de recherche français ou étrangers, des laboratoires publics ou privés.

Screening and polaronic effects induced by a metallic gate and a surrounding oxide on donor and acceptor impurities in silicon nanowires

Cite as: J. Appl. Phys. **103**, 073703 (2008); <https://doi.org/10.1063/1.2901182>

Submitted: 24 September 2007 • Accepted: 21 January 2008 • Published Online: 01 April 2008

Mamadou Diarra, Christophe Delerue, Yann-Michel Niquet, et al.



View Online



Export Citation

ARTICLES YOU MAY BE INTERESTED IN

[Single donor induced negative differential resistance in silicon n-type nanowire metal-oxide-semiconductor transistors](#)

Journal of Applied Physics **107**, 093703 (2010); <https://doi.org/10.1063/1.3399999>

[Quantum confinement in Si and Ge nanostructures: Theory and experiment](#)

Applied Physics Reviews **1**, 011302 (2014); <https://doi.org/10.1063/1.4835095>

[Ab-initio study of the segregation and electronic properties of neutral and charged B and P dopants in Si and Si/SiO₂ nanowires](#)

Journal of Applied Physics **118**, 104306 (2015); <https://doi.org/10.1063/1.4930048>



Applied Physics
Reviews

Read. Cite. Publish. Repeat.

19.162
2020 IMPACT FACTOR*



Screening and polaronic effects induced by a metallic gate and a surrounding oxide on donor and acceptor impurities in silicon nanowires

Mamadou Diarra,¹ Christophe Delerue,^{1,a)} Yann-Michel Niquet,² and Guy Allan¹

¹*Institut d'Electronique, de Microélectronique et de Nanotechnologie (UMR CNRS 8520),
Département ISEN, 41 Boulevard Vauban, F-59046 Lille Cedex, France*

²*Institute for Nanosciences and Cryogenics (INAC), SP2M/L_Sim, CEA Grenoble,
38054 Grenoble Cedex 9, France*

(Received 24 September 2007; accepted 21 January 2008; published online 1 April 2008)

We present self-consistent tight binding calculations of the electronic structure of donor and acceptor impurities in silicon nanowires surrounded by a gate oxide (SiO_2 or HfO_2) and a metallic gate. These environments efficiently screen the potential of the impurities so that their ionization energy strongly decreases with respect to the case of freestanding nanowires. It is also shown that the carriers trapped by the impurities form a polaron due to the response of the ions in the surrounding oxide layer. We predict that the polaron shift represents a large part of the impurity ionization energy, in particular, in HfO_2 . Our work demonstrates the importance of screening and polaronic effects on the transport properties in nanoscale devices based on Si nanowires. © 2008 American Institute of Physics. [DOI: 10.1063/1.2901182]

I. INTRODUCTION

Recent progress in bottom-up fabrication techniques^{1–4} have fostered the interest in semiconductor nanowires as promising building blocks for future nanoelectronics. As the channel length of metal-oxide-semiconductor field effect transistors reaches the nanometer scale, silicon nanowires (SNWs) can be used in new types of devices such as gate-all-around transistors,^{5–7} in which short channel effects are reduced thanks to a better gate control.⁸ Semiconductor nanowires are also investigated for many other applications in optoelectronics, quantum electronics, chemical, and biosensing.² In parallel, important efforts are engaged to understand the fundamental properties of these nanoobjects.

In this context, we have recently calculated the electronic structure of donor and acceptor impurities, in order to address the problem of doping in SNWs.⁹ We have shown that the ionization energy of the impurities is largely enhanced in freestanding nanowires compared to the bulk, in such a way that it becomes difficult to ionize them in small wires. This effect is a consequence of the so-called dielectric confinement^{10,11} which appears when there is an important mismatch between the dielectric constant of the nanowire and of its surrounding.

In this paper, we consider donor and acceptor impurities in SNWs covered by an oxide layer (SiO_2 or HfO_2) and surrounded by a metallic gate (Fig. 1), i.e., in typical situations encountered in Si-based nanodevices such as gate-all-around transistors. We show that the electronic properties of the impurities are considerably modified by these environments. First, the metallic gate and the oxide layer tend to screen the impurity potential leading to a strong reduction of their ionization energy. Second, the carrier (electron or hole) bound to the impurity forms a polaron due to the displace-

ment of the ions of the surrounding oxide matrix in response to the electric field induced by the carrier itself. We present electronic structure calculations showing that the polaron shift represents a large part of the impurity binding energy.

The paper is organized as follows. First, we describe the physics of the polaron formation when the SNW is covered by an oxide layer and we present the self-consistent tight binding calculations used in this work. Second, we discuss the ionization energy of the donor and acceptor impurities in different environments, and we provide analytical expressions for practical use.

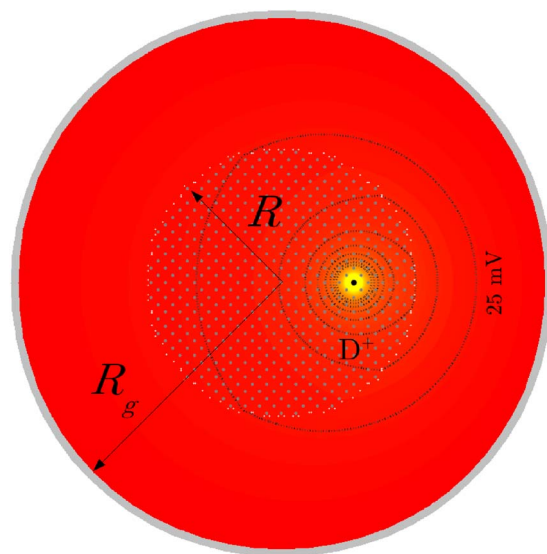


FIG. 1. (Color online) Schematic of the nanowire device structure considered in this work. The silicon nanowire with radius R is embedded in SiO_2 or HfO_2 and possibly surrounded by a metallic gate with radius R_g . The potential created by an ionized donor impurity (D^+) is plotted as an illustration ($R=5$ nm, $R_g=10$ nm). The spacing between equipotential lines is 25 mV.

^{a)}Electronic mail: christophe.delerue@isen.fr.

II. METHODOLOGY

A. Polaron formation

Ionized donor (acceptor) impurities in semiconductors induce a long-range Coulomb potential in which the electron (hole) can be trapped. In the bulk, this potential is efficiently screened so that all the impurities are ionized at room temperature. In small nanowires (radius R of 10 nm), the situation is different because the screening depends on the dielectric constant ϵ_{out} of the surrounding material, the ionization energy of the impurities increasing when ϵ_{out} decreases.⁹ Dielectric effects were already invoked by Chazalviel *et al.* to explain why dry and wet porous silicons have very different transport and optical properties, the polar solvent (water) playing the role of a dielectric medium in the wet configuration.¹² But it was shown in that work that polaronic states are formed, which complicates the picture significantly. We will show in the following that polaronic effects are important not only for SNWs embedded in an electrolyte¹² but also in more common and technologically important situations where SNWs are covered by conventional oxides (SiO_2 or HfO_2).

Let us consider a SNW modeled as a cylinder of dielectric constant ϵ_{in} ($=11.7$ for Si) embedded in an oxide with dielectric constant ϵ_{out} . We will neglect, in a first approximation, the dynamics of the ions in the oxide (which is much slower than the dynamics of the electrons), and therefore use a model in which ϵ_{out} can take two values,^{12,13} ϵ_{out}^0 and $\epsilon_{\text{out}}^\infty$. The *static* dielectric constant ϵ_{out}^0 contains both the ionic and electronic responses, while the *dynamical* dielectric constant $\epsilon_{\text{out}}^\infty$ only contains the electronic contribution, which means that $\epsilon_{\text{out}}^\infty$ is evaluated at a frequency above the highest optical phonon modes of the oxide.

We consider the electronic structure of the system in two situations, when an electron (hole) is free in the SNW or when it is trapped by an impurity. Working in a single-electron picture, the Hamiltonian is written $H=H_0+V$, where V contains the different terms coming from the dielectric polarization of the system, including the lattice relaxation of the ions in the surrounding oxide. Under the above assumptions, the electronic and nuclear motions can be separated (Born–Oppenheimer approximation), so that V is a function of the normal coordinates Q that describe the displacements of the ions.¹¹ Hence, we can visualize the problem in a configuration coordinate diagram (Fig. 2) that represents the energy of the system in the trapped state [$E_{\text{trap}}(Q)$] and in the delocalized state [$E_{\text{free}}(Q)$] versus Q . As a result of the electron-lattice interaction, $E_{\text{trap}}(Q)$ and $E_{\text{free}}(Q)$ have a minimum at different coordinates Q_{trap} and Q_{free} , respectively. The ionization energy is the difference between the two minima, $E_I=E_{\text{free}}(Q_{\text{free}})-E_{\text{trap}}(Q_{\text{trap}})$. We also define the vertical transition energy $\Delta E(Q)=E_{\text{free}}(Q)-E_{\text{trap}}(Q)$, which is the energy required to ionize the carrier keeping all the ions at a fixed configuration Q . Vertical transitions take place in optical processes, following the Franck–Condon principle.^{11,12} For example, after optical excitation of a trapped carrier, the ions are left in the configuration Q_{trap} immediately after the transition, and then relax progressively to the equilibrium configuration Q_{free} . Figure 2 shows that

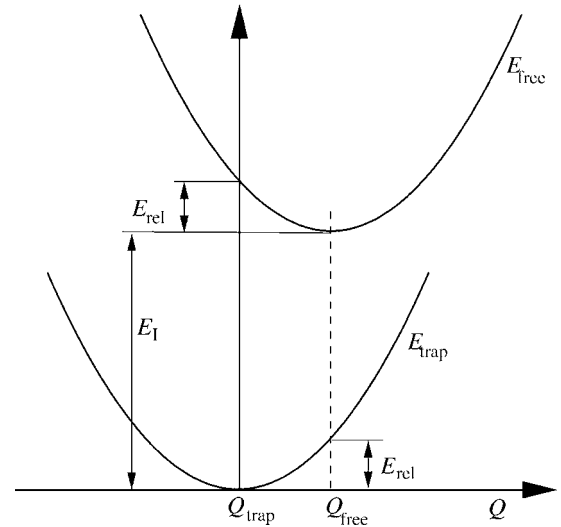


FIG. 2. Configuration coordinate diagram showing the variation of the total energy of the system with respect to a configuration coordinate Q that represents the displacement of the ions in the oxide surrounding the nanowire. Two configurations are considered: (1) the impurity is ionized, the carrier is free in the band (E_{free}); (2) the carrier is trapped by the impurity (E_{trap}). E_I is the ionization energy and E_{rel} is the energy of relaxation (polaron shift) when the system reaches its stable configuration after a vertical transition.

the relaxation energy is $E_{\text{rel}}=[\Delta E(Q_{\text{trap}})-\Delta E(Q_{\text{free}})]/2$, assuming that $E_{\text{trap}}(Q)$ and $E_{\text{free}}(Q)$ have the same parabolic behavior.¹⁴

Therefore, we have just to calculate $\Delta E(Q_{\text{trap}})$ and $\Delta E(Q_{\text{free}})$ to determine the ionization energy using $E_I=\Delta E(Q_{\text{free}})+E_{\text{rel}}=[\Delta E(Q_{\text{trap}})+\Delta E(Q_{\text{free}})]/2$.¹⁵ The interest of this approach is that $\Delta E(Q_{\text{trap}})$ and $\Delta E(Q_{\text{free}})$ are vertical transition energies which are simple differences between eigenvalues of the single-particle Hamiltonian H with V determined at a fixed atomic configuration. Thus, it remains to calculate the energy of the trapped state and of the extended state in configurations Q_{trap} and Q_{free} . When the carrier is in an extended state, its energy does not depend on the impurity potential. $V(r)$ only contains the interaction between the carrier and the polarization charges induced by its own presence at the interface between the wire and its surrounding.^{10–13,16} Due to the velocity of the carrier (and following our assumptions about the dynamics of the ions),¹² only the electronic component of the dielectric response contributes to this term,¹⁷ which can be introduced in $V(\mathbf{r})$ as a self-energy potential $\Sigma(\mathbf{r})=\pm\frac{1}{2}\lim_{\mathbf{r}'\rightarrow\mathbf{r}}V_{\text{image}}^\infty(\mathbf{r},\mathbf{r}')$ (+ for an electron, – for a hole). $V_{\text{image}}^\infty(\mathbf{r},\mathbf{r}')$ is the image charge potential equal to $V^\infty(\mathbf{r},\mathbf{r}')-V_{\text{bulk}}(\mathbf{r},\mathbf{r}')$, where $V^\infty(\mathbf{r},\mathbf{r}')$ is the energy of a charge $+e$ at \mathbf{r} in the electrostatic potential created by a charge $+e$ at \mathbf{r}' in the SNW, and $V_{\text{bulk}}(\mathbf{r},\mathbf{r}')=e^2/\epsilon_{\text{in}}|\mathbf{r}-\mathbf{r}'|$ is the same quantity but in the bulk semiconductor.⁹ The symbol ∞ means that all the potentials are calculated using $\epsilon_{\text{out}}=\epsilon_{\text{out}}^\infty$. The effects of the self-energy on the SNW band structure are discussed in Ref. 16.

The situation for the trapped carrier is more complicated, $V(\mathbf{r})$ being the sum of the potentials induced by the ionized impurity and by the carrier itself. The impurity nucleus being immobile, its contribution to $V(\mathbf{r})$ is simply given by the static response $V_{\text{imp}}(\mathbf{r})=\pm V^0(\mathbf{r}_{\text{imp}},\mathbf{r})$, where \mathbf{r}_{imp} is the impurity position, the sign $+(-)$ holds for an acceptor (donor),

and V^0 is calculated with $\epsilon_{\text{out}} = \epsilon_{\text{out}}^0$. The potential induced by the carrier itself is once again the self-energy potential $\Sigma(\mathbf{r})$ that describes the fast electronic component of the dielectric response. Thus, in the configuration Q_{free} , the trapped state is an eigenstate of H with $V(\mathbf{r}) = V_{\text{imp}}(\mathbf{r}) + \Sigma(\mathbf{r})$. In the configuration Q_{trap} , the ions in the oxide also contribute to the potential. Then $V(\mathbf{r})$ becomes $V_{\text{imp}}(\mathbf{r}) + \Sigma(\mathbf{r}) \pm \int |\psi(\mathbf{r}')|^2 [V_{\text{image}}^0(\mathbf{r}, \mathbf{r}') - V_{\text{image}}^\infty(\mathbf{r}, \mathbf{r}')] d\mathbf{r}'$ (+ for an electron, - for a hole), assuming that the ions respond to the (static) time-averaged charge density $\pm e|\psi(\mathbf{r})|^2$, where $\psi(\mathbf{r})$ is the localized state.¹⁸

B. Tight binding calculations

The electronic structure of the SNWs is calculated in a semiempirical tight binding (TB) framework because it represents a method of choice to study semiconductor nanostructures¹¹ and shallow impurities from bulk semiconductors¹⁹ to nanostructures.⁹ This atomistic approach reproduces the complex band structure of the semiconductor and takes into account the impurity chemical shifts, as required to calculate impurity ionization energies or confinement energies with accuracy. The methodology of the TB calculations is described in Refs. 9 and 16, but the dependence of $V(\mathbf{r})$ on the wave function $\psi(\mathbf{r})$ requires to solve the Schrödinger equation in a self-consistent way, complicating the problem significantly. The Hamiltonian H_0 is written in a $sp^3d^5s^*$ basis set.²⁰ The potentials and self-energies are computed as the solutions of Poisson equation using either a finite difference approach or a Fourier–Bessel expansion,¹⁶ in the cylindrical geometry of Fig. 1. A metallic gate with radius R_g (taken as the reference of potentials $V_g = 0$) can be added around the nanowire to simulate gate-all-around geometries. We take $\epsilon_{\text{out}}^0 = 26.17$ and $\epsilon_{\text{out}}^\infty = 5.37$ for HfO_2 ,²¹ $\epsilon_{\text{out}}^0 = 3.9$ and $\epsilon_{\text{out}}^\infty = 2.1$ for SiO_2 , and $\epsilon_{\text{in}} = 11.7$ for Si.

III. RESULTS AND DISCUSSIONS

A. Nanowires embedded in SiO_2

Figure 3 presents E_I versus R in the case of a P impurity at the center of SNWs and compares the situations where the wires are in vacuum or are embedded in SiO_2 ($R_g \rightarrow \infty$). The surrounding oxide screens the impurity potential leading to an important reduction of E_I . Similar results are obtained for other types of donors (As, Sb) or acceptors (B), as well as for impurities placed at different positions. This is evidenced in Fig. 3 for P donors located at a distance $R/2$ from the axis of the nanowires. The weak dependence of the ionization energy on the impurity position is due to the fact that the image charge potential is almost constant in a dielectric cylinder.⁹ These results show that the thermal ionization of the carriers is favored by the presence of the oxide, although it remains unlikely in the smallest wires. At room temperature, for $R = 5$ nm and a doping density N_d of 10^{18} cm^{-3} , we predict a doping efficiency (probability of ionization) of 47% in SiO_2 compared to 6% in vacuum (a general expression of the free carrier concentration versus E_I and N_d is given in Ref. 22. Figure 3 also shows that the polaron effect is far from being negligible: E_{rel} represents $\sim 15\%$ of E_I and is greater than 17 meV for $R < 5$ nm.

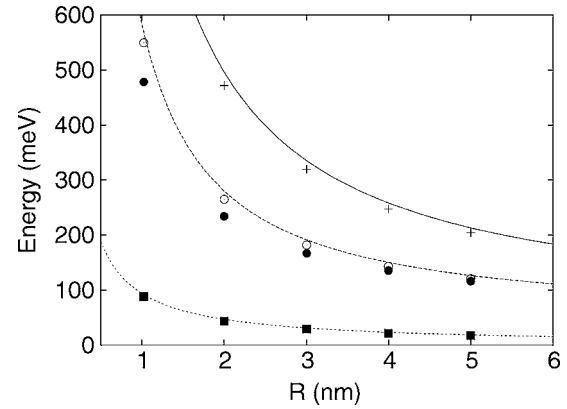


FIG. 3. Ionization energy E_I of a P impurity placed at the center of a Si nanowire with respect to its radius R . The nanowire is either in vacuum (+) or embedded in SiO_2 (o). E_{rel} (■), the energy of relaxation of the ions in SiO_2 when the electron is trapped by the impurity, contributes significantly to the ionization energy. The lines show that E_I and E_{rel} can be approximated by $E_I \approx E_I^0 + E_{\text{conf}} + (U^\infty + U^0)/2$ and $E_{\text{rel}} \approx (U^\infty - U^0)/2$, where E_I^0 is the ionization energy in bulk Si (45 meV), E_{conf} is the contribution coming from the quantum confinement (Ref. 9), and U^0 (U^∞) is the image charge potential calculated with the static (dynamical) dielectric constant of the oxide. The ionization energy calculated for impurities placed at a distance $R/2$ from the axis of the nanowires is shown for comparison (●).

We have established an analytical expression of E_I using the same arguments as in our previous work.⁹ We use the fact that the image charge potential $V_{\text{image}}(\mathbf{r}, \mathbf{r}')$ can be approximated by a constant independent of the positions and given by $U = (2/\epsilon_{\text{in}}R)(\epsilon_{\text{in}} - \epsilon_{\text{out}})/(\epsilon_{\text{in}} + \epsilon_{\text{out}})F(\epsilon_{\text{in}}/\epsilon_{\text{out}})$ when $|\mathbf{r} - \mathbf{r}'| \ll R$, with $F(x) = 0.0949x^3 + 17.395x^2 + 175.739x + 200.674)/(x^2 + 50.841x + 219.091)$ (eV nm).^{9,16} Using $\langle \psi | V_{\text{image}}^0(\mathbf{r}_{\text{imp}}, \mathbf{r}) | \psi \rangle \approx U^0$ (U calculated with $\epsilon_{\text{out}} = \epsilon_{\text{out}}^0$), the vertical transition energy $\Delta E(Q_{\text{free}})$ is close to $E_I^0 + E_{\text{conf}} + U^0$, where E_I^0 is the ionization energy in bulk Si and E_{conf} is the quantum confinement energy (determined with $\epsilon_{\text{out}} = \epsilon_{\text{in}}$).²³ The carrier self-energy $\Sigma(\mathbf{r})$ coming from the fast electronic response does not contribute to E_I because it is approximately the same in the bound state as in the extended state.⁹ Similarly, the vertical transition energy $\Delta E(Q_{\text{trap}})$ is close to $E_I^0 + E_{\text{conf}} + U^\infty$ because there is an almost complete cancellation between the terms coming from $V_{\text{imp}}(\mathbf{r})$ and $\pm \int |\psi(\mathbf{r}')|^2 V_{\text{image}}^0(\mathbf{r}, \mathbf{r}') d\mathbf{r}'$ in $V(\mathbf{r})$, the total charge carried by the impurity nucleus and the trapped electron or hole being zero. From these expressions of $\Delta E(Q_{\text{trap}})$ and $\Delta E(Q_{\text{free}})$, we deduce $E_I \approx E_I^0 + E_{\text{conf}} + (U^\infty + U^0)/2$ and $E_{\text{rel}} \approx (U^\infty - U^0)/2$. Figure 3 shows that the analytical expressions of E_I and E_{rel} agree well with the TB values.

B. Nanowires embedded in HfO_2

When SNWs are embedded in HfO_2 (Fig. 4), E_I is further reduced due to a more efficient dielectric screening of the impurity potential. At room temperature, for $R = 5$ nm and $N_d = 10^{18} \text{ cm}^{-3}$, we predict a doping efficiency of 78% much higher than in vacuum (6%). The importance of polaronic effects, however, increases (E_{rel} represents $\sim 25\%$ of E_I for $R < 6$ nm) due to the ionic character of HfO_2 . Figure 4 shows that the analytical expressions of E_I and E_{rel} agree once again very well with the TB values. Using these expressions, we predict for $R = 10$ nm an ionization energy of

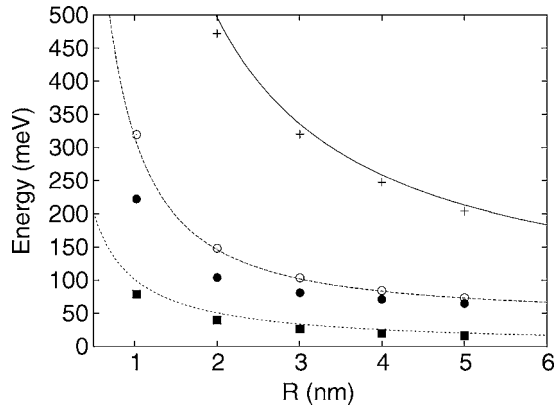


FIG. 4. Same as Fig. 2 but for Si nanowires embedded in HfO₂.

56 meV close to the bulk value (45 meV) and a polaron shift of 10 meV in HfO₂ (83 and 9 meV in SiO₂, respectively). This example proves that polaronic effects must be considered even in large nanowires. As a matter of fact, E_I remains larger than the bulk value E_I^0 even if $\epsilon_{\text{out}}^0 > \epsilon_{\text{in}}$ (that is, $U^0 < 0$) because the polaron shift $E_{\text{rel}} \approx (U^\infty - U^0)/2$ is still greater than $|U^0|$ for the present value of $\epsilon_{\text{out}}^\infty$.

C. Effect of a metallic gate

The effect of a metallic gate surrounding the SNWs is shown in Fig. 5. The gate tends to screen the impurity potential so that E_I becomes closer to its bulk value and that the impurities are easily ionized at room temperature. The influence of the gate becomes negligible only when its radius R_g is much larger than R , which shows that the screening is actually very efficient in cylindrical geometry. This result emphasizes the need to take into account long-range Coulomb interactions in nanoscale electronic devices. Figure 5 shows that E_I is still given by $E_I \approx E_I^0 + E_{\text{conf}} + (U^\infty + U^0)/2$, but with U now calculated with the gate. U can be written

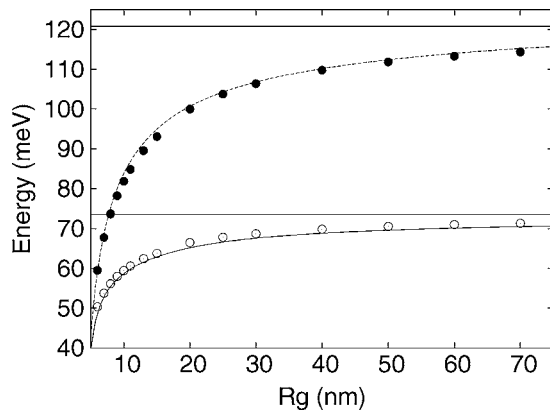


FIG. 5. Ionization energy E_I of a P impurity placed at the center of a Si nanowire of radius $R=5$ nm as function of the radius R_g of the metallic gate. The material between the nanowire and the gate is either SiO₂ (●) or HfO₂ (○). The lines show that E_I can be approximated by $E_I \approx E_I^0 + E_{\text{conf}} + (U^\infty + U^0)/2$ where E_I^0 is the ionization energy in bulk Si (45 meV), E_{conf} is the contribution coming from the quantum confinement (Ref. 9), and U^0 (U^∞) is the image charge potential calculated with the static (dynamical) dielectric constant of the oxide. The horizontal lines indicate the ionization energy in the configurations without metallic gate ($R_g \rightarrow \infty$).

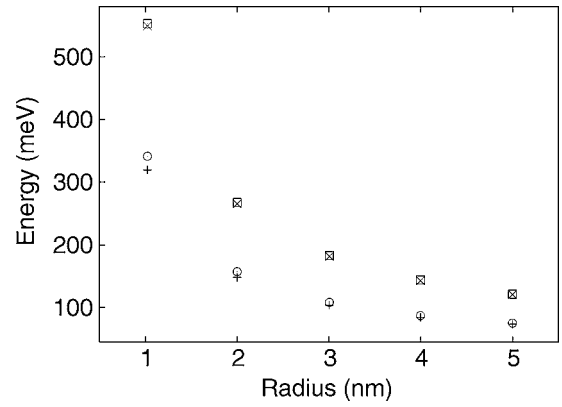


FIG. 6. Ionization energy E_I of a P impurity placed at the center of a Si nanowire embedded in SiO₂ (×, □) and HfO₂ (+, ○) with respect to the radius R . The results are obtained using two different assumptions for the trapped state: (1) the ions only respond to the average charge density (+, ×); (2) they instantaneously respond to the electronic displacements (□, ○).

$U = (1/\epsilon_{\text{in}}R)g(R/R_g, \epsilon_{\text{in}}/\epsilon_{\text{out}})$, where $g(x, y)$ has been calculated along the line of Ref. 16 and is given in Ref. 24.

D. Influence of the dynamical response of the ions in the trapped state

Up to now, we have assumed that the ions only respond to the average charge density $\pm e|\psi(\mathbf{r})|^2$ in the trapped state. However, it might not be fully justified to neglect the dynamical response of the ions in the trapped state,²⁵ because the highest phonon energy in the oxides (~ 150 meV in SiO₂)²⁶ is comparable to the ionization energy E_I . In order to assess the validity of our approximation, we have considered the opposite and extreme situation where the ions would be able to follow instantaneously the displacements of the trapped carrier. In that case, the previous formalism, which neglects the dynamical response of the ions, cannot be applied anymore. The potential seen by the trapped carrier actually becomes $V(\mathbf{r}) = V_{\text{imp}}(\mathbf{r}) \pm \frac{1}{2} \lim_{\mathbf{r}' \rightarrow \mathbf{r}} V_{\text{image}}^0(\mathbf{r}, \mathbf{r}')$ (+ for an electron, - for a hole), where the second term is just the self-energy calculated using $\epsilon_{\text{out}} = \epsilon_{\text{out}}^0$. In this limit, the ionization energy is the difference between the single-particle energy levels of the trapped and free states.¹⁷ One then easily recovers the previous expression for the ionization energy, $E_I \approx E_I^0 + E_{\text{conf}} + (U^\infty + U^0)/2$, using once again the fact that $V_{\text{image}}^0(\mathbf{r}, \mathbf{r}')$ is almost constant inside the nanowire. This conclusion is supported by the full TB calculation (Fig. 6), which shows that the ionization energy is almost the same in the two approximations. We therefore conclude that the inclusion of the exact dynamical response of the ions would have a small influence on the results.

IV. CONCLUSION

In conclusion, we show that the electronic properties of donor and acceptor impurities in SNWs are deeply modified by their environment, in particular, in the presence of metallic gates or gate oxides commonly used in microelectronics technology (SiO₂, HfO₂). Whereas the doping efficiency is strongly reduced when SNWs are in vacuum because the impurity ionization energy is enhanced,⁹ we predict a much higher efficiency when SNWs are embedded in a material

which tends to screen the impurity potential. These results open the possibility to engineer the conductivity of the nanowires by playing with their environment. In the case of SNWs surrounded by an oxide layer, we show that polaronic effects must be considered, in particular when the oxide is an ionic material such as HfO_2 . Polaronic effects are important even in 20 nm thick wires which are now easily produced by growth techniques.²

Polaronic effects should also be significant in the case of carriers localized by potential or size fluctuations. They might increase the effective mass of the free carriers even in weakly disordered systems. These effects are likely to occur in nanoscale electronic devices based on silicon technology, and their consequences on the transport properties have to be explored in future studies. It is already clear from our work that the scattering potential at the origin of the diffusive transport is not intrinsic to the nanowires because it is strongly dependent on their environment. Thus the transport properties of nanowires result from the subtle interplay between not only band structure and disorder effects but also polaronic states, which requires us to include the response of the ions in a self-consistent way.

ACKNOWLEDGMENTS

This work was supported by the French ‘‘Action Concertée Incitative’’ (ACI) ‘‘Transnanofils.’’ Y.M.N. acknowledges support from the European Integrated Project (IP) NODE (EU Contract No. 015783 NODE).

¹Y. Cui, Z. H. Zhong, D. L. Wang, W. U. Wang, and C. M. Lieber, *Nano Lett.* **3**, 149 (2003).

²C. M. Lieber, *MRS Bull.* **28**, 486 (2003).

³P. Yang, *MRS Bull.* **30**, 85 (2005).

⁴A. B. Greytak, L. J. Lauhon, M. S. Gudiksen, and C. M. Lieber, *Appl. Phys. Lett.* **84**, 4176 (2004).

⁵G. Pei, J. Kedsierski, P. Oldiges, M. Jeong, and E. C. C. Kan, *IEEE Trans. Electron Devices* **49**, 1411 (2002).

⁶P. Colinge, *Solid-State Electron.* **48**, 897 (2004).

⁷M. Bescond, J. L. Autran, D. Munteanu, and M. Lannoo, *Solid-State Electron.* **48**, 567 (2004).

⁸Y. Taur and T. H. Ning, *Fundamentals of Modern VLSI Devices* (Cambridge University Press, Cambridge, 1998).

⁹M. Diarra, Y.-M. Niquet, C. Delerue, and G. Allan, *Phys. Rev. B* **75**,

045301 (2007).

¹⁰L. V. Keldysh, *Superlattices Microstruct.* **4**, 637 (1966).

¹¹C. Delerue and M. Lannoo, *Nanostructures—Theory and Modelling* (Springer-Verlag, Berlin, 2004).

¹²J.-N. Chazalviel, F. Ozanam, and V.-M. Dubin, *J. Phys. I* **4**, 1325 (1994).

¹³L. E. Brus, *Phys. Rev. B* **53**, 4649 (1996).

¹⁴This approximation is the usual one in theory of electron-lattice coupling (Ref. 11) and is also fully justified by Fig. 6 of Ref. 12 showing that (1) $E_{\text{trap}}(Q)$ and $E_{\text{free}}(Q)$ are parabolic functions of Q and (2) $\Delta E(Q)$ is linear (see also the appendix of that paper).

¹⁵The method used in Ref. 12 to calculate E_l is basically equivalent to ours because $E_{\text{trap}}(Q)$ and $E_{\text{free}}(Q)$ are parabolic functions of Q (Ref. 14).

¹⁶Y.-M. Niquet, A. Lherbier, N. H. Quang, M. V. Fernández-Serra, X. Blase, and C. Delerue, *Phys. Rev. B* **73**, 165319 (2006).

¹⁷We neglect possible polaronic effects when the carrier is ionized in the bands (free polaron). We expect polaronic effects to be much smaller for extended states than for localized ones. However, due to its one dimensional character, the polaronic couplings in the bands would be worth more detailed investigations which are beyond the scope of the present paper.

¹⁸In contrast to self-energy term, the factor of 1/2 does not apply here since we consider the potential induced by the ions as external to the electronic system, $V(\mathbf{r})$ being the single-electron potential of the electronic equation in the Born–Oppenheimer approximation.

¹⁹A. S. Martins, J. G. Menchero, R. B. Capaz, and B. Koiller, *Phys. Rev. B* **65**, 245205 (2002).

²⁰B. Boykin, G. Klimeck, and F. Oyafuso, *Phys. Rev. B* **69**, 115201 (2004).

²¹G.-M. Rignanese, X. Gonze, G. Jun, K. Cho, and A. Pasquarello, *Phys. Rev. B* **69**, 184301 (2004).

²²We have obtained that the free carrier density n in a SNW doped with donor impurities at a concentration N_d can be safely approximated by the same expression as in the bulk semiconductor: $n = (N_c/4)(-1 + \{1 + [(8N_d/N_c)]e^{E_f/kT}\}^{1/2})e^{-E_f/kT}$ where N_c is the bulk effective density of states in the conduction band $[N_c = (M/\sqrt{2})(m^*kT/\pi\hbar^2)^{3/2}]$, m^* being the effective mass and M corresponding to the number of conduction band minima. We can obtain the hole density similarly.

²³For donors in SNWs, an expression of E_{conf} is given in Ref. 9, in the caption of Fig. 2.

²⁴ $g(x, y)$ is a function (eV nm) given by $g(x, y) = (a + bx + cy + dx^2 + exy + fy^2 + gx^3 + hx^2y + ixy^2 + jy^3 + kx^4 + lx^3y + mx^2y^2 + nxy^3 + oy^4) / (a_1 + b_1x + c_1y + d_1x^2 + e_1xy + f_1y^2 + g_1x^3 + h_1x^2y + i_1xy^2 + y^3 + k_1x^4 + l_1x^3y + m_1x^2y^2 + n_1xy^3)$, where $a = -401.348$, $b = 1107.763$, $c = 49.87$, $d = -6710.873$, $e = -10572.34$, $f = 316.688$, $g = 11593.92$, $h = 1619.274$, $i = 8365.34$, $j = 34.600$, $k = -5975.533$, $l = -2133.74$, $m = -9238.82$, $n = -23.957$, $o = 0.1898$, $a_1 = 219.091$, $b_1 = 604.74$, $c_1 = 269.932$, $d_1 = -3663.54$, $e_1 = 7266.26$, $f_1 = 51.841$, $g_1 = 6329.25$, $h_1 = 809.637$, $i_1 = 598.338$, $k_1 = -3262.11$, $l_1 = -3202.65$, $m_1 = 42.722$, and $n_1 = -6.616$.

²⁵The angular frequency for the rotation of the carrier around the impurity nucleus is of the order of the highest phonon frequencies, in the 10^{14} s^{-1} range.

²⁶P. H. Gaskell and D. W. Johnson, *J. Non-Cryst. Solids* **20**, 171 (1976).